Front. Optoelectron. China 2009, 2(3): 293–298
DOI 10.1007/s12200-009-0013-0

RESEARCH ARTICLE

# Tapered photonic crystal fiber for supercontinuum generation in telecommunication windows

**Yongzhao XU (✉)[1], Zhixin CHEN[2], Hongtao LI[1], Yanfen WEI[3]**

1 Department of Electronic Engineering, Dongguan University of Technology, Dongguan 523808, China
2 School of Information, Central University of Finance and Economics, Beijing 100081, China
3 Tianjin Mobile Communications Corporation, Tianjin 300021, China



**Abstract** We numerically studied supercontinuum generation in a tapered photonic crystal fiber with flattened dispersion properties. The fiber was weakly tapered to have normal dispersion at wavelengths around 1.55 μm after a certain distance. We pumped 4 ps pulses with low peak power and found that flatly broadened, wideband supercontinuum was generated in telecommunication windows. Furthermore, we also demonstrated the effects of tapered length and pulse width of the pump pulse on supercontinuum generation.

**Keywords** fiber optics, photonic crystal fiber, dispersion, supercontinuum

## 1 Introduction

With the development of photonic crystal fibers (PCFs), supercontinuum (SC) generation has been the focus of intense research in recent years and PCFs were proven to be successful media for efficient SC generation [1–6]. Ultra-wideband light sources based on SC generation have applications in various fields such as optical coherence tomography, spectroscopy, and frequency metrology. SC used in optical communication is another attractive application. There has been increasing interest in applying SC sources to wavelength-division-multiplexing (WDM) optical transmission systems, for which multi-channel of SC pulse train are modulated as carrier waves [7–11]. To enhance WDM networks with higher bit rates and longer transmission distances, further research to improve the flatness of the SC is needed. The requirement can be met by optimizing the design of the SC fiber and the pumping condition.

Received November 17, 2008; accepted December 3, 2008

E-mail: xuyongzhao@gmail.com

PCFs, also called holey fibers or microstructured fibers, commonly consist of a fused silica core surrounded by a regular array of air holes running along the fiber length. They have the advantage of design flexibility in controlling the mode propagation properties. By varying the arrangement and size of the air holes, the fiber dispersion can be tailored in broad ranges [12–17]. Therefore, PCFs offer the possible design of SC fiber which is suitable for flat wideband SC generation in telecommunication windows and meets the requirement of WDM. Previous theoretical and experimental results have demonstrated that flat SC generation in the 1.55-μm region can be achieved using dispersion-flattened PCFs together with picosecond pulse [3,8,13,18]. But in order to generate an ultra-broadband SC using those PCFs, a much high pump power and a short input pulse width are required.

In this paper, we focus on PCF design for flat wideband SC generation in telecommunication windows. A novel PCF characterized by flattened chromatic dispersion which also gradually moves from anomalous dispersion to normal dispersion with increasing fiber length is proposed. The numerical result shows that the proposed PCF offers the possibility of flat and efficient SC generation in telecommunication windows using a few picosecond pulses with low pump peak power.

## 2 Theoretical models

Here we combine the advantageous properties of PCF and tapering to design a dispersion-flattened and decreasing PCF. A design procedure is summarized as the following steps: firstly, a PCF with appropriate air-hole pitch ($\Lambda$) and air-hole diameter ($d$) is chosen for achieving flattened anomalous dispersion properties in the 1.55-μm region; secondly, tapering is used to gradually decrease the fiber dispersion and move the dispersion from a positive value to a negative one.

We consider a triangular PCF with $\Lambda$= 2.6 μm and $d$ = 0.632 μm. While tapering the PCF, we assume that the ratio of air-hole diameter to air-hole pitch $d/\Lambda$ (also called relative hole size) is constant. We consider the case that $\Lambda$ linearly decreases, which is expressed as

$$\Lambda(z) = \Lambda_0 - \frac{\Lambda_0 - \Lambda_t}{L} z, \tag{1}$$

where $\Lambda_0$ is the initial air-hole pitch, $\Lambda_t$ is the final air-hole pitch at the end of the taper, and $L$ is the tapered length.

We calculate the chromatic dispersion of the fiber using a full-vectorial modal solver [19]. Figure 1 shows the chromatic dispersion profiles along the taper with $\Lambda$ varying from 2.6 to 2.4 μm. As can be seen, the PCF has flattened dispersion behavior in the 1.55-μm region, and the chromatic dispersion also decreases along the taper with decreasing pitch. At the wavelength of 1.55 μm, chromatic dispersion at the input is 7.9 ps/(nm·km)$^{-1}$ and it decreases to 0 when $\Lambda$= 2.428 μm; for $d < 2.428$ μm, the chromatic dispersion becomes negative (normal dispersion). Figure 2 shows the chromatic dispersion at 1.55 μm versus pitch.

From the dispersion profiles, we can obtain the dispersion coefficients $\beta_m$ and then fit the $\Lambda$-variation of each $\beta_m$ with a polynomial to obtain an analytical formula for $\beta_m$. Figure 3 shows the terms $\beta_2$–$\beta_5$ at 1.55 μm as a function of $\Lambda$.

We use a generalized scalar nonlinear Schrödinger equation (NSE) to model the broad-band pulse propagation in the PCF, written as [20]

$$\frac{\partial A}{\partial z} + \frac{\alpha}{2} A - \sum_{m=2}^{\infty} \frac{i^{m+1} \beta_m}{m!} \frac{\partial^m A}{\partial T^m} = \mathrm{i}\gamma \left(1 + \frac{\mathrm{i}}{\omega_0} \frac{\partial}{\partial T}\right) \left[A(z,T) \int_{-\infty}^{T} R(T - T') |A(z,T')|^2 \mathrm{d}T'\right], \tag{2}$$

where i is an imaginary number; $A$ is the electric field amplitude; $z$ is the longitudinal coordinate along the fiber; $T$ is the time in a reference frame traveling with the pump pulse; $\beta_m$ is the $m$th-order dispersion coefficient at the central frequency $\omega_0$; $\alpha$ is the fiber loss; $\gamma = n_2\omega/(cA_{\mathrm{eff}})$ is the nonlinear coefficient, where $n_2$ is the nonlinear refractive-index coefficient of the fiber and $A_{\mathrm{eff}}$ is the effective mode-field area. The equation allows for modeling the propagation of pulses with spectral widths comparable with the central frequency $\omega_0$. The nonlinear effects of self-phase modulation (SPM), self-steepening, and Raman scattering are described by the term on the right hand side, where $R(\tau)$ is the Raman response function and the time derivative is responsible for the self-steepening. Equation (2) has been solved using the split-step Fourier method and the following numerical results are based on Eq. (2). In the simulations, the effect of dispersion

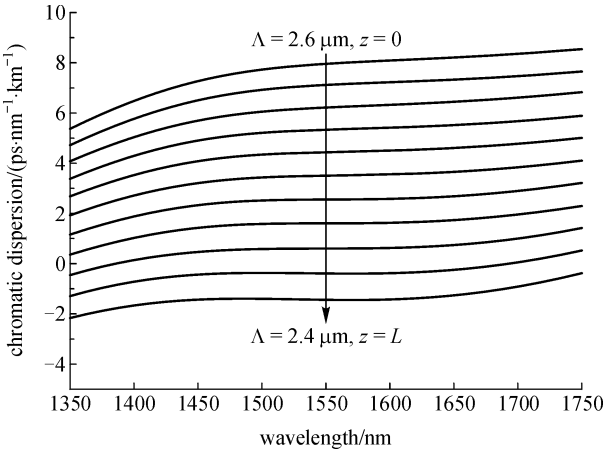


**Fig. 1** Chromatic dispersion profiles of tapered PCF with air-hole pitch $\Lambda$ decreasing from 2.6 to 2.4 μm

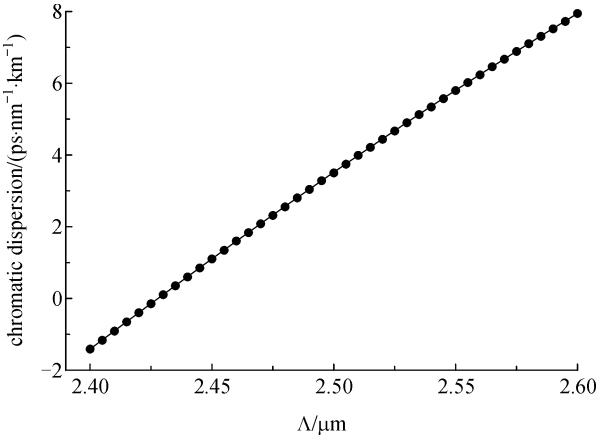


**Fig. 2** Chromatic dispersion at wavelength of 1.55 μm versus air-hole pitch $\Lambda$

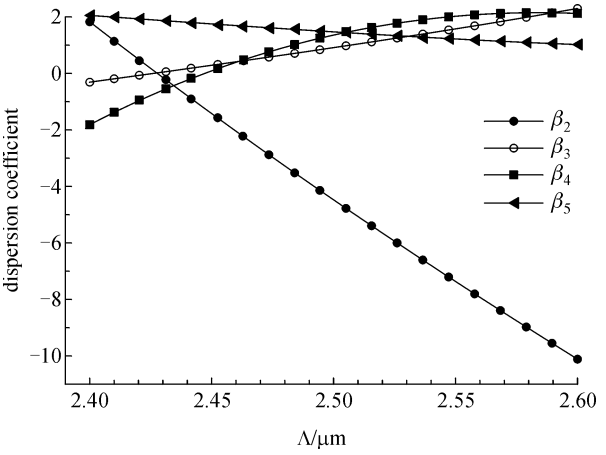


**Fig. 3** Dispersion coefficients $\beta_2$/(ps$^2$·km$^{-1}$), $\beta_3$/(10$^{-2}$ ps$^3$·km$^{-1}$), $\beta_4$/(10$^{-5}$ ps$^4$·km$^{-1}$), and $\beta_5$/(10$^{-6}$ ps$^5$·km$^{-1}$) versus air-hole pitch $\Lambda$

was found to be accurate using terms up to $\beta_8$, with higher-order terms having negligible influence. Because of weak tapering, the variation of $A_{\text{eff}}$ along the taper is neglected for simplicity.

The pump pulses are assumed to have hyperbolic secant shape:

$$A(0,\tau) = \sqrt{P_0}\sec h(T/T_0), \tag{3}$$

where $P_0$ is the peak power and $T_0$ is related to the full width at half maximum (FWHM) by $T_{\text{FWHM}} \approx 1.763T_0$.

## 3 Numerical results and analysis

We first consider the case that the tapered length of the PCF is $L = 0.2$ km. The input pulses have a duration of 4 ps FWHM and a central wavelength of 1.55 μm. The effective peak power which is defined as the product of peak power $P_0$ and nonlinear coefficient $\gamma$ is $\gamma P_0 = 24.48\ \text{km}^{-1}$. For simplicity, the fiber loss was neglected and its effects are discussed below.

The simulated SC is shown in Fig. 4. It is an ultra-broadband SC that covers the S-band (1460–1530 nm), C-band (1530–1565 nm), and L-band (1565–1625 nm). The SC is flat and smooth over a few hundreds of nanometers. As reported in Refs. [3,8,13,18], flat SC can also be generated in telecommunication windows using dispersion flattened PCFs with small normal dispersion. But in order to generate an ultra-broadband SC, a much high effective peak power and a short input pulse width are required.

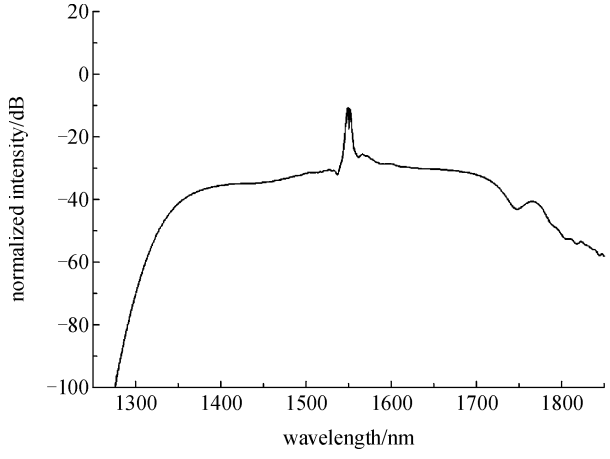


**Fig. 4** SC generated from tapered PCF

To investigate how the SC generates, it is helpful to view the evolution of pump pulse and its spectrum. Figures 5(a) and 5(b) show respectively the pulse evolution and the 30-dB spectrum width with propagation distance increasing. There are three stages of SC generation. At the first stage of propagation below distance $L_0$ that is defined as the propagation distance at which the chromatic dispersion

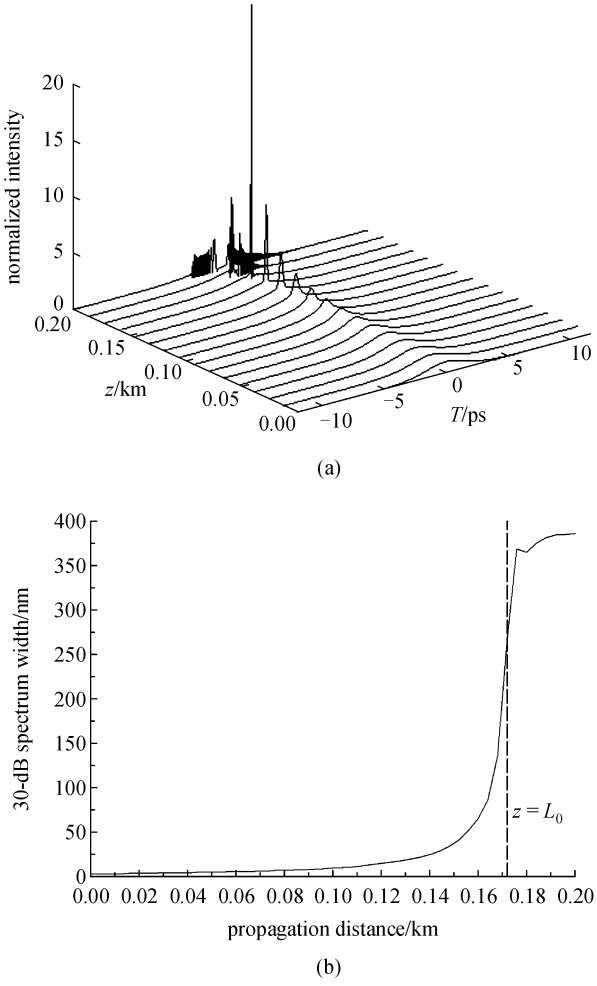


**Fig. 5** Evolution of pump pulse along fiber. (a) Temporal evolution; (b) evolution of 30-dB spectrum width along propagation distance, where dashed line indicates the distance of $L_0$

decreases to 0 (for tapered length $L = 0.2$ km, $L_0 = 0.172$ km), the spectrum broadens because of pulse compression process in the anomalous dispersion region, but the spectrum width increases slowly with propagation. At the second stage, the propagation distance is in the vicinity of $L_0$, the peak power of the pulse has increased greatly, and thereby high nonlinear effects drastically extend the spectrum to an SC. Figure 6 shows the spectral evolution in the vicinity of $L_0$. SPM is believed to be the dominant nonlinear effect responsible for the spectral broadening. After $z = L_0$, although more and more spectra fall into the normal dispersion region, the spectrum continues to broaden because the pulse is still intense enough to produce nonlinearity. In this process, the spectrum becomes flatter because of the combined effects of nonlinearity and the normal dispersion. At the third stage, most of the spectra fall into the normal dispersion region after $z = 1.1L_0$, the pulse breaks up, and the spectrum almost ceases to change. The generation of the flat SC is summarized as the following stages: initial

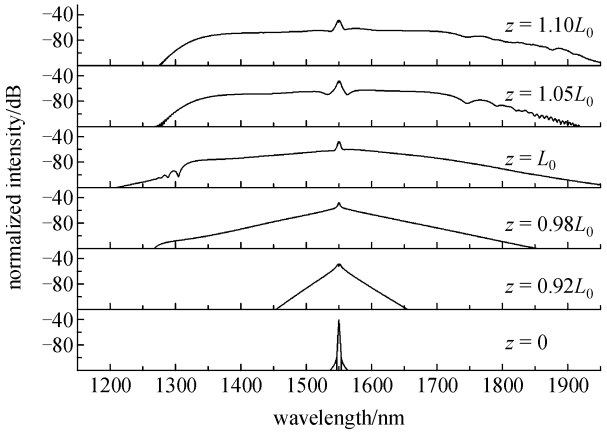


**Fig. 6** Spectral evolution in vicinity of $L_0$

spectral broadening caused by pulse compression and a subsequent spectral flattening caused by the transition from a nonlinear wave to a dispersive wave.

In the spectral evolution, we note that the spectrum broadens in a nearly symmetrical manner before $z = 0.92L_0$, after which with further decrease in the chromatic dispersion, higher-order dispersion plays an increasingly important role in the SC generation. The spectrum exhibits asymmetric spectral broadening as a result of higher-order dispersion, Raman scatting, and self-steepening.

The tapered length of the fiber has much influence on SC generation. For given pitch $\Lambda_0$ and $\Lambda_t$, a longer tapered length requires a lower input peak power for generating a flat wideband SC. It can be understood from the nature of soliton compression that the longer tapered length makes it more efficient for compressing the pump pulse. For comparison, Fig. 7 shows the variation of the minimum effective peak power of the pump pulses for generating a flat wideband SC with tapered length from 0.1 to 1 km. The duration $T_{\mathrm{FWHM}}$ of the pump pulses is constant at 4 ps. It is evident that a short tapered length requires a much higher effective peak power at the input, but by choosing an appropriate tapered length the required effective peak power for generating a flat wideband SC will become much lower.

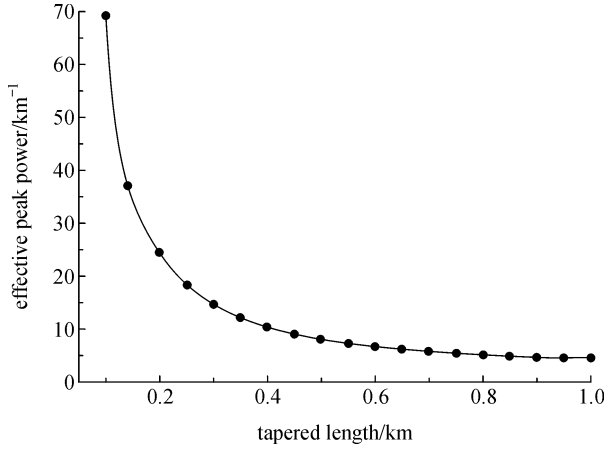


**Fig. 7** Minimum effective peak powers of pump pulses for generating flat wideband SC versus tapered length of PCF

The fiber works well for a wide range of input pulse widths. Figure 8 illustrates the generated SCs when the input pulse widths are 0.5 ps (a), 1 ps (b), 2 ps (c), 4 ps (d), 6 ps (e), and 8 ps (f), and the corresponding effective peak powers are 73.36 $\mathrm{km^{-1}}$ (a), 32.20 $\mathrm{km^{-1}}$ (b), 20.30 $\mathrm{km^{-1}}$ (c), 24.48 $\mathrm{km^{-1}}$ (d), 37.26 $\mathrm{km^{-1}}$ (e), and 55.60 $\mathrm{km^{-1}}$ (f), respectively. It can be seen from the figure that when the input pulse is shorter, two grooves in the spectrum are formed at the two sides of the pump wavelength. As the pulse width increases, the grooves gradually disappear. An SC with optimal flatness can be obtained by appropriately choosing the input pulse width and pump peak power.

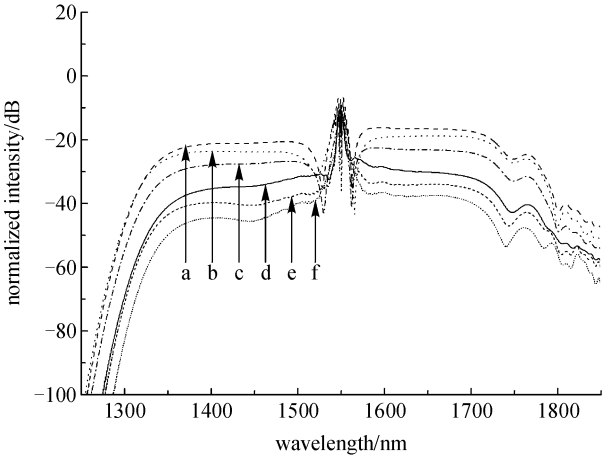


**Fig. 8** Generated SCs for different input pulse width

In the above discussions, we simulated SC generations in the absence of fiber loss ($\alpha$). Actually it cannot be neglected for a long fiber length. For a constant pump condition, if fiber loss exceeds a certain degree, the power of the pulse decays before spectral broadening and flattening, and consequently a flatly broadened spectrum is no longer generated. We calculated the spectrum included fiber loss under the same pump condition as those in Fig. 4. Figure 9 illustrates the change of 30-dB spectrum width for different values of $\alpha$. We note that the spectrum width decreases rapidly with $\alpha$ increasing, but after $\alpha$ reaches a certain value, and spectrum width decreases more slowly than previously because SC is no longer generated. When fiber loss is included, it is also possible to generate a flat SC with an identical width as that of $\alpha = 0$, but it requires a pump pulse with higher peak power. We change the effective peak power of the pump pulse for different values of fiber loss so as to keep the same spectrum width as that of $\alpha = 0$. The results are also shown in Fig. 9, which indicates that the effective peak

powers of the input pulses nearly linearly increase with fiber loss increasing.

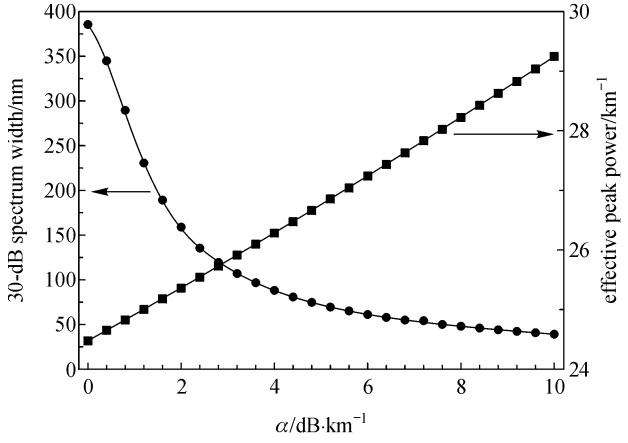


**Fig. 9** 30-dB spectrum width and effective peak power of pump pulses versus fiber loss

## 4 Conclusion

In conclusion, a new technique to control dispersion in PCFs is proposed to design a tapered PCF for flat SC generation. The numerical results show that it is possible to design a PCF with flattened chromatic dispersion which also gradually moves from anomalous dispersion to normal dispersion with increasing fiber length, and this fiber can be used for flat and efficient SC generation in the telecommunication windows.

**Acknowledgements** This work was supported by the Foundation for Key Program of Ministry of Education, China (No. 104046).

## References

1. Ravi Kanth Kumar V V, George A K, Reeves W H, Knight J C, Russell P St J. Extruded soft glass photonic crystal fiber for ultrabroad supercontinuum generation. Optics Express, 2002, 10 (25): 1520–1525
2. Yu Y Q, Ruan S C, Du C L, Yao J Q. Spectral broadening in the 1.3 μm region using a 1.8-m-long photonic crystal fiber by femtosecond pulses from an optical parametric amplifier. Acta Photonica Sinica, 2005, 34(4): 481–484 (in Chinese)
3. Xu Y Z, Ren X M, Wang Z N, Zhang X, Huang Y Q. Flat supercontinuum generation at 1550 nm in a dispersion-flattened microstructure fibre using picosecond pulse. Chinese Physics Letters, 2007, 24(3): 734–737
4. Hu M L, Wang Q Y, Li Y F, Wang Z, Zhang Z G, Chai L, Zhang R B. Experimental analysis of the dependence factor during supercontinuum generation in photonic crystal fiber. Acta Physica Sinica, 2004, 53(12): 4243–4247 (in Chinese)
5. Yu Y Q, Ruan S C, Du C L, Yao J Q. Supercontinuum generation using a polarization-maintaining photonic crystal fibre by a regeneratively amplified Ti:sapphire laser. Chinese Physics Letters, 2005, 22(2): 384–387
6. Kudlinski A, George A K, Knight J C, Travers J C, Rulkov A B, Popov S V, Taylor J R. Zero-dispersion wavelength decreasing photonic crystal fibers for ultraviolet-extended supercontinuum generation. Optics Express, 2006, 14(12): 5715–5722
7. Ohara T, Takara H, Yamamoto T, Masuda H, Morioka T, Abe M, Takahashi H. Over-1000-channel ultradense WDM transmission with supercontinuum multicarrier source. Journal of Lightwave Technology, 2006, 24(6): 2311–2317
8. Xu Y Z, Ren X M, Wang Z N, Zhang X, Huang Y Q. Flatly broadened supercontinuum generation at 10 Gbit/s using dispersion-flattened photonic crystal fibre with small normal dispersion. Electronics Letters, 2007, 43(2): 87–88
9. Yusoff Z, Petropoulos P, Furusawa K, Monro T M, Richardson D J. A 36-channel × 10-GHz spectrally sliced pulse source based on supercontinuum generation in normally dispersive highly nonlinear holey fiber. IEEE Photonics Technology Letters, 2003, 15(12): 1689–1691
10. Nakasyotani T, Toda H, Kuri T, Kitayama K. Wavelength-division-multiplexed millimeter-waveband radio-on-fiber system using a supercontinuum light source. Journal of Lightwave Technology, 2006, 24(1): 404–410
11. Lee J H, Kim C H, Han Y G, Lee S B. WDM-based passive optical network upstream transmission at 1.25 Gb/s using Fabry-Pérot laser diodes injected with spectrum-sliced, depolarized, continuous-wave supercontinuum source. IEEE Photonics Technology Letters, 2006, 18(17–20): 2108–2110
12. Wu W Q, Chen X W, Zhou H, Zhou K F, Lin X S, Lan S. Investigation of the ultraflattened dispersion in photonic crystal fibers with hybrid cores. Acta Photonica Sinica, 2006, 35(1): 109–113 (in Chinese)
13. Saitoh K, Koshiba M. Highly nonlinear dispersion-flattened photonic crystal fibers for supercontinuum generation in a telecommunication window. Optics Express, 2004, 12(10): 2027–2032
14. Wu T L, Chao C H. A novel ultraflattened dispersion photonic crystal fiber. IEEE Photonics Technology Letters, 2005, 17(1); 67–69
15. Matsui T, Nakajima K, Sankawa I. Dispersion compensation over all the telecommunication bands with double-cladding photonic-crystal fiber. Journal of Lightwave Technology, 2007, 25(3): 757–762
16. Liu J G, Xue L F, Wang Z, Kai G Y, Liu Y G, Zhang W G, Dong X Y. Large anomalous dispersion at short wavelength and modal properties of a photonic crystal fiber with large air holes. IEEE Journal of Quantum Electronics, 2006, 42(9): 961–968
17. Ju J, Jin W, Suleyman Demokan M. Design of single-polarization single-mode photonic crystal fiber at 1.30 and 1.55 μm. Journal of Lightwave Technology, 2006, 24(2): 825–830
18. Yamamoto T, Kubota H, Kawanishi S, Tanaka M, Yamaguchi S. Supercontinuum generation at 1.55 μm in a dispersion-flattened polarization-maintaining photonic crystal fiber. Optics Express, 2003, 11(13): 1537–1540

19. Saitoh K, Koshiba M. Full-vectorial imaginary-distance beam propagation method based on finite element scheme: application to photonic crystal fibers. IEEE Journal of Quantum Electronics, 2002, 38(7): 927–933
20. Agrawal G P. Nonlinear Fiber Optics. 2nd ed. New York: Academic Press, 1995